Proceedings of Science and Mathematics
Faculty of Science, Universiti Teknologi Malaysia
Vol. 23, 2024, page 8-16

Epidemiology Model of Influenza A (H1N1) Transmission in Ashanti Region of Ghana

Nurshahadah Azrin, Fuaada Mohd Siam
Department of Mathematical Sciences, Faculty of Science, Universiti Teknologi Malaysia
Corresponding author: fuaada@utm.my

Abstract
Influenza A (H1N1) is an infectious viral illness caused by RNA virus belonging to the family *Orthomyxoviridae*. A compartmental epidemiology model, the Susceptible-Exposed-Infectious-Recovered (SEIR) model was developed to study the transmission of influenza A (H1N1) using population data from the Ashanti region of Ghana. The SEIR model is based on Ordinary Differential Equations (ODEs) to track the flow of individuals but different disease state. The stability of the model is obtained using the Routh-Hurwitz Stability Criterion method. The study also calculated the basic reproduction number, R_0 by using the Next-Generation Method. This parameter helps us understand how influenza A (H1N1) spreads within the environment. The obtained value was R_0 greater than 1, indicating that the virus will continue circulating and not die out. Furthermore, the SEIR model was simulated using the ODE45 built-in function in MATLAB. Numerical simulations were conducted by adjusting certain parameter values and comparing the result. These numerical finding could assist in implementing strategies to confront and limit the spread of influenza A (H1N1) as quickly as possible.
Keywords: Influenza A (H1N1); SEIR Model; Basic reproduction number, R_0 ; Numerical simulations.

1 Introduction

Influenza, commonly known as the flu, is a viral infection affecting the respiratory system caused by influenza viruses from the family Orthomyxoviridae, which includes seven genera such as Alphainfluenzavirus and Betainfluenzavirus [1]. Influenza viruses are categorized into four types; A, B, C and D, distinguished by two key proteins, hemagglutinin (HA) and neuraminidase (NA) [2]. Influenza A and B are responsible for seasonal epidemics in humans, with type A being the most dangerous and prone to pandemics. This study focuses on Influenza A (H1N1), a highly contagious virus spread through respiratory droplets and contaminated surfaces, causing symptoms similar to seasonal flu. Severe cases can lead to pneumonia and death, especially in individuals with weakened immune systems.

Influenza A (H1N1) is highly contagious, spreading rapidly through respiratory droplets from coughs or sneezes, and indirectly via contaminated surfaces like doorknobs [3]. Symptoms mirror those of seasonal flu, including fever, cough, sore throat, body aches, headache, chills, and fatigue. Severe cases can result in pneumonia, respiratory failure, and death, especially in individuals with underlying health conditions or weakened immune systems [4].

Over a million people were infected with the H1N1 virus globally, according to the World Health Organisation (WHO) [4]. The Ashanti Region experienced its first H1N1 pandemic on August 31, 1918, spreading from a ship from Freetown, Sierra Leone, and resulting in at least 100,000 deaths in Ghana [5]. To prevent and treat influenza A (H1N1), understanding the disease's behaviour is crucial. Implementing prevention methods and reducing fatalities require mathematical modelling and data analysis. This study uses the Susceptible-Exposed-Infectious-Recovered (SEIR) epidemiological model to analyse influenza A (H1N1) transmission and better understand its spread. The basic reproduction number, R_0, will be calculated using the Next-Generation Matrix method. When $R_0 > 1$, The epidemic increases exponentially, which means that one infected individual infects more than one individual on average. Meanwhile, when $R_0 < 1$ shows that the disease will surely die out without affecting a large share of the population. Therefore, the research is done in the hope that the SEIR model can be used as a reference model for influenza A (H1N1) spread.

2 Literature Review

2.1 Epidemiology of the Pandemic Influenza A (H1N1)

The first outbreak of influenza A (H1N1) occurred in April 2009 in La Gloria, Veracruz, Mexico, where an unusual number of influenza-like-illness cases were reported as early as March 5, 2009 [6]. By April 12, the WHO requested verification of the suspected outbreak, which affected 28.5% of La Gloria's population between March 5 and April 10 [7]. Severe pneumonia cases were soon reported in Mexico City and San Luis Potosi, prompting the government to increase national surveillance and collaborate with international health organizations. The virus quickly spread worldwide, marking the first major influenza pandemic since 1969 [7].

Following the initial outbreak, the WHO declared a "public health emergency of international concern" on April 25, 2009, as the virus spread to multiple countries [8]. Canada reported its first cases on April 26, with an early outbreak at a Nova Scotia private school linked to students who had travelled to Mexico. By May 1, 11 countries, including New Zealand, Israel, and the UK, reported confirmed cases [9]. The virus spread to Europe, Hong Kong, and Korea by May 2, with Mexico reporting 397 cases and 16 deaths, and Canada reporting 165 confirmed cases by May 6. By this time, 23 countries had reported at least one pandemic H1N1 case [10].

2.2 Factors Affecting the Transmission of Influenza A (H1N1)

Influenza viruses spread primarily through aerosol particles produced when infected individuals cough, sneeze, talk, or breathe. Large droplets settle quickly on surfaces, while smaller particles (<5 μm) can stay airborne longer and travel further, penetrating deeply into the respiratory tract [11]. Environmental factors like temperature and humidity also influence virus transmission, with cold and humid conditions favouring the spread in winter.

Social behaviour plays a key role in influenza spread. Close contact in crowded indoor settings, especially schools, increases transmission risk [12]. Children are effective transmitters due to their close interactions. Promoting hand hygiene, respiratory etiquette, social distancing, and vaccination in schools can help reduce influenza transmission.

2.3 High-Risk Groups for Influenza A (H1N1)

Individuals in high-risk groups, such as pregnant women, young children, and those with chronic health conditions, are more susceptible to severe outcomes from Influenza A (H1N1). Pregnant women face increased risk due to changes in their immune and respiratory systems, leading to complications like pneumonia and adverse outcomes for the fetus, including preterm birth and low birth weight. Children under 5 years old are at high risk because their immune systems are still developing, making them more vulnerable to severe symptoms and respiratory infections [13].

Individuals with chronic health conditions, such as heart disease, diabetes, and weakened immune systems, are more likely to experience severe complications from H1N1, including pneumonia and worsening of their existing conditions. The virus puts additional strain on their compromised systems, increasing the likelihood of severe illness and even death.

3 Methodology

3.1 Formulation of the SEIR Model

This section discussed the derivation of the extended SIR model for the influenza A (H1N1). The extended SIR model is called as Suspected-Exposed-Infected-Recovered (SEIR). The SEIR model derivation and the stability analysis of the model will be carried out throughout this section. The SEIR model on the spread of influenza A (H1N1) is divided into four compartments, namely Suspected (S), Exposed (E), Infected (I), and Recovered (R). N is the total population size. Individuals in an infected class can cause other individuals to become infected. The SEIR model is presented schematically in Figure 1. The model is based on the work of Okyere, S. et al. [14].

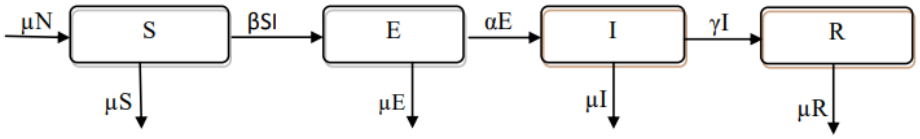

Figure 1: Schematic diagram of compartments of the influenza A (H1N1) model

Based on the flow diagram in Figure 1, the rate of change in the number of individuals which are Susceptible, Exposed, Infected and Recovered over time in SEIR model of the spread of influenza A (H1N1) can be represented as follows:

$$\frac{dS}{dT} = \mu - (\mu + \beta I)S, \tag{1}$$

$$\frac{dE}{dT} = \beta IS - (\mu + \alpha)E, \tag{2}$$

$$\frac{dI}{dT} = \alpha E - (\Upsilon + \mu)I, \tag{3}$$

$$\frac{dR}{dT} = \Upsilon I - \mu R. \tag{4}$$

Definition of parameters of SEIR model for COVID-19 is presented in Table 1.

Table 1: Definition of parameters

Parameter	Definition
μ	The birth and death rate
β	The transmission rate
α	The latent rate
ϒ	The recovery rate

3.2 Stability Analysis of SEIR Model

3.2.1 Equilibrium Points

The equilibrium points that will be considered in this study are the disease-free equilibrium point (DFEP) to produce R_0 that will be used to determine the spread of influenza A (H1N1). Therefore, the endemic equilibrium point (EEP) is omitted in this work. To determine the equilibrium points, each equation in Equation (1)-(4) must be equal to zero.

3.2.2 Disease-Free Equilibrium Point (DFEP)

The disease-free equilibrium point (DFEP) is where there is no spread of COVID-19 in which $E = I = 0$. Hence, the DFEP are as follow:

$$(s, e, i, r) = (1, 0, 0, 0).$$

3.2.3 Endemic Equilibrium Point (EEP)

At endemic equilibrium point (EEP), it I assumed that there are individuals who have been exposed to the disease and are infected in which $E \neq 0$ and $I \neq 0$. Hence, the EEP are as follow:

$$(s*, e*, i*, r*) = \left(\frac{1}{R_0}, \frac{\mu(R_0-1)}{R_O(\mu+\alpha)}, \frac{\mu(R_0-1)}{\beta}, \frac{\Upsilon(R_0-1)}{\beta}\right).$$

3.3 Stability Analysis at Disease-Free Equilibrium Point (DFEP)

To determine the stability analysis of the equilibrium point at DFEP, the SEIR model needs to be linearized by using Jacobian matrix. Based on Equation (1)-(4), the Jacobian matrix is given as:

$$J = \begin{bmatrix} -\mu-\beta i & 0 & -\beta s & 0 \\ \beta i & -(\mu+\alpha) & \beta s & 0 \\ 0 & \alpha & -(\Upsilon+\mu) & 0 \\ 0 & 0 & \Upsilon & -\mu \end{bmatrix} \quad (5)$$

The eigenvalues are determined, and the characteristic equation is as follows:

$$\lambda^4 + \lambda^3(4\mu+\Upsilon+\alpha) + \lambda^2(6\mu^2+3\alpha\mu+3\mu\Upsilon+\alpha\Upsilon+\beta\alpha) + \lambda(2\alpha\beta\mu+2\alpha\Upsilon\mu+3\alpha\mu^2+3\Upsilon\mu^2+4\mu^3) + \mu^2(\alpha\beta+\alpha\Upsilon+\mu\alpha+\Upsilon\mu+\mu^2) = 0.$$

Where, $a_1 = \lambda^3, a_2 = \lambda^2, a_3 = \lambda$ and $a_4 = \mu^2(\alpha\beta+\alpha\Upsilon+\mu\alpha+\Upsilon\mu+\mu^2)$, hence

$$a_1 = (4\mu+\Upsilon+\alpha) \quad (6)$$
$$a_2 = (6\mu^2+3\alpha\mu+3\mu\Upsilon+\alpha\Upsilon+\beta\alpha) \quad (7)$$
$$a_3 = \mu[(\mu+\alpha)(2\alpha\beta\mu+2\alpha\Upsilon\mu+3\alpha\mu^2+3\Upsilon\mu^2+4\mu^3)(\mu+\Upsilon)-\beta\alpha] \quad (8)$$
$$a_4 = \mu^2(\alpha\beta+\alpha\Upsilon+\mu\alpha+\Upsilon\mu+\mu^2) \quad (9)$$

From Routh-Hurwitz stability criterion, if $a_1 > 0, a_4 > 0, a_1a_2a_3 - a_4 > 0$, then the equilibrium point (DFEP) is stable. Hence obtain that $R_0 < 1$.

3.4 Stability Analysis at Endemic Equilibrium Point (EEP)

To determine the stability analysis of the equilibrium point EEP, the SEIR model needs to be linearized by using Jacobian matrix. Based on Equation (1)-(4), the Jacobian matrix is given as:

$$J = \begin{bmatrix} -\mu R_0 & 0 & -\frac{\beta s}{R_0} & 0 \\ \mu(R_0-1) & -(\mu+\alpha) & \frac{\beta s}{R_0} & 0 \\ 0 & \alpha & -(\Upsilon+\mu) & 0 \\ 0 & 0 & \Upsilon & -\mu \end{bmatrix} \quad (10)$$

The eigenvalues are determined, and the characteristic equation is as follows:

$$\lambda^4 + \lambda^3(3\mu+\Upsilon+\alpha+\mu R_0) + \lambda^2(\alpha\Upsilon+2\alpha\mu+\mu R_0+2\Upsilon\mu+\Upsilon R_0+3\mu^2+3\mu^2R_0-\alpha\beta) + \lambda(\Upsilon\alpha\mu+\Upsilon\alpha R_0+\Upsilon\mu^2+2\Upsilon\mu^2R_0+\alpha\mu^2+2\alpha R_0+\mu^3+3\mu^2R_0-\alpha\beta\mu) + (\Upsilon\alpha\mu^2R_0+\Upsilon\mu^3R_0+\alpha\mu^3R_0+\mu^4R_0) = 0.$$

Where, $b_1 = \lambda^3, b_2 = \lambda^2, b_3 = \lambda$ and $b_4 = \Upsilon\alpha\mu^2R_0+\Upsilon\mu^3R_0+\alpha\mu^3R_0+\mu^4R_0$, hence

$$b_1 = 3\mu+\Upsilon+\alpha+\mu R_0 \quad (11)$$
$$b_2 = \alpha\Upsilon+2\alpha\mu+\mu R_0+2\Upsilon\mu+\Upsilon R_0+3\mu^2+3\mu^2R_0-\alpha\beta \quad (12)$$
$$b_3 = \Upsilon\alpha\mu+\Upsilon\alpha R_0+\Upsilon\mu^2+2\Upsilon\mu^2R_0+\alpha\mu^2+2\alpha R_0+\mu^3+3\mu^2R_0-\alpha\beta\mu \quad (13)$$
$$b_4 = \Upsilon\alpha\mu^2R_0+\Upsilon\mu^3R_0+\alpha\mu^3R_0+\mu^4R_0 \quad (14)$$

and the characteristics equation becomes

$$\lambda^4 + b_1\lambda^3 + b_2\lambda^2 + b_3\lambda + b_3 = 0. \quad (15)$$

From Routh-Hurwitz stability criterion, if $b_1 > 0, b_4 > 0, b_1 b_2 b_3 - b_4 > 0$, are true then all roots of the characteristic equation have negative real parts which means a stable equilibrium. Thus, the endemic equilibrium point is stable when $R_0 > 1$ by the Routh-Hurwitz criteria.

3.5 Basic Reproduction Number, R_0

The R_0 of the SEIR model is determined using the Next-Generation Matrix method [6]. The DFEP for the model is utilized to complete the calculation of R_0. Matrix **F** represents the rate of appearance of new infections in different compartments, while matrix **V** represents the rate of transfer of individuals from one compartment to another.

First, we need to regroup the system of ODEs into disease classes and non-disease classes. However, only the disease class were used to find matrix **F** and **V**. Therefore, matrix F and V are computed as follow:

$$\boldsymbol{F} = \begin{bmatrix} 0 & \beta s \\ 0 & 0 \end{bmatrix},$$

$$\boldsymbol{V} = \begin{bmatrix} (\mu + \alpha) & 0 \\ -\alpha & (\Upsilon + \mu) \end{bmatrix}.$$

Then, calculate the Next-Generation matrix of the system and evaluate the spectral radius if the matrix to obtain R_0.

$$\boldsymbol{FV^{-1}} = \begin{bmatrix} \frac{\beta\alpha}{(\mu+\alpha)(\Upsilon+\mu)} & \frac{\beta}{(\Upsilon+\mu)} \\ 0 & 0 \end{bmatrix}.$$

Hence, taking the largest eigenvalues from the matrix

$$|\boldsymbol{FV^{-1}}| = \begin{vmatrix} \frac{\beta\alpha}{(\mu+\alpha)(\Upsilon+\mu)} & \frac{\beta}{(\Upsilon+\mu)} \\ 0 & 0 \end{vmatrix}.$$

The basic reproduction number is as follow

$$R_0 = \frac{\beta\alpha}{(\mu+\alpha)(\Upsilon+\mu)}.$$

The R_0 of the system (1)-(4) is locally asymptotically stable if $R_0 < 1$ and unstable if $R_0 > 1$.

4 Numerical Simulation of SEIR Model of Influenza A (H1N1)

The simulation of the SEIR model will be obtained using MATLAB. Several simulations are carried out by adjusting the parameters to understand the transmission dynamics of the influenza A (H1N1). To perform the numerical simulations, the initial conditions are taken as $S(0) = 4725042, E(0) = 2, I(0) = 2$ and $R(0) = 0$ and the parameters values used in this study are shown on Table 2 [11].

Table 2: Parameter values of SEIR model

Parameter	Definition	Value
μ	The birth and death rate	0.0088
β	The transmission rate	0.3016
α	The latent rate	0.5
ϒ	The recovery rate	0.2857
N	Population of Ashanti Region	4725046

Figure 2 presents the SEIR model, illustrates the transmission dynamics of diseases under specific initial parameters. The green curve initially reflects a high number of susceptible individuals gradually declining as more people become exposed and infected over time. The red curve represents the population of exposed individuals, which rapidly increases as susceptible individuals contract the disease, peaks, and subsequently declines as they transition into the infected class. Similarly, the pink curve illustrates the actively infected population, reaching its peak as a significant number of individuals spread the disease and then gradually decreases as recoveries occur. Lastly, the blue curve represents the number of individuals who have recovered from the disease, steadily increasing until it reaches its maximum, indicating a substantial portion of the population has successfully overcome the disease and acquired immunity.

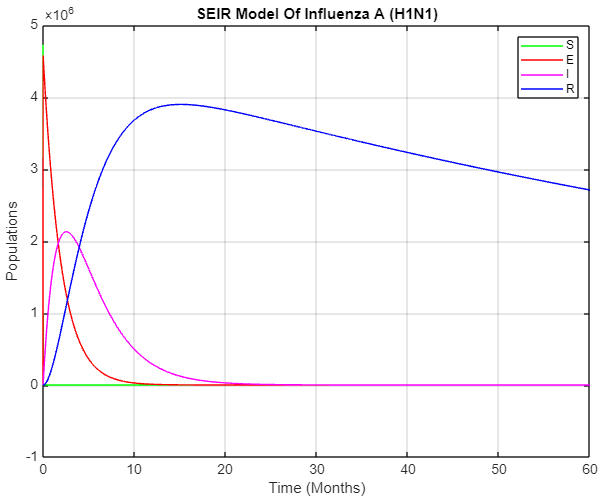

Figure 2 SEIR model for $\mu = 0.0088, \beta = 0.3016, \alpha = 0.5, \Upsilon = 0.2857$.

4.1 Changes in Transmission Rate (β)

The changes in the transmission rate, β is explained where the parameters of β is changed to observe the spread of influenza A (H1N1) in the infected population. The transmission rate varies as parameters of β changed from 0.3016 to 0.3245 and then increase to 0.4000. However, the remaining the parameters are same as previous simulation: μ = 0.0088, α = 0.5 and Υ = 0.2857.

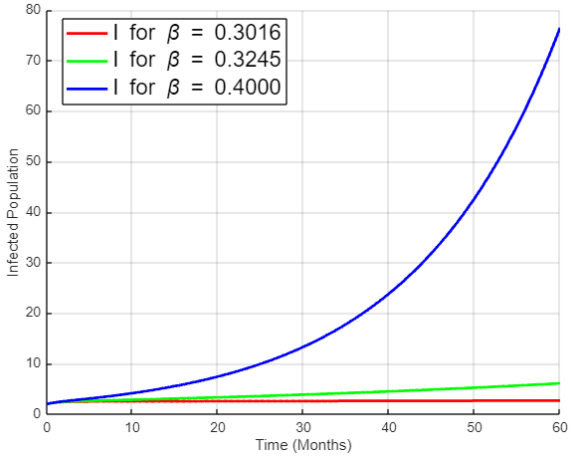

Figure 3 The total number of infected individuals for β = 0.3016, β = 0.3245 and β = 0.4000.

In Figure 3, it can be seen that if the transmission rate, β increases, the number of infected individuals also increases. This is because a higher transmission rate means that the disease spreads more

quickly, and leading to a larger number of people getting infected. The red curve (β = 0.3016) represents a low transmission rate and the infected individuals decrease accordingly. Conversely, when the blue curve (β = 0.4000) represents a higher transmission rate and the infected individuals increases rapidly.

4.2 Changes in Latent Rate (α)

By changing the parameter value of latent rate, α, the variation of dynamics can be observed. The simulation results can be compared with varying the parameter values of α = 0.5000, α = 1.000 and α = 1.5000. The result is shown in Figure 4.

Figure 4 shows that the infected population over time for different values of α, which represent the latent rate. The latent rate is the rate at which infected individuals become infectious. A higher latent rate (α) means a faster transition from infected to infectious. This is reflected in the Figure 4, where the blue curve (α = 1.5) shows the fastest growth in infected population, indicating individuals quickly become infectious. The red line (α = 0.5) shows the slowest growth, indicating individuals take longer to become infectious. The green line (α = 1) falls somewhere in between. The shape of the curves suggests that even with a slower latent rate (lower α), the infected population eventually grows.

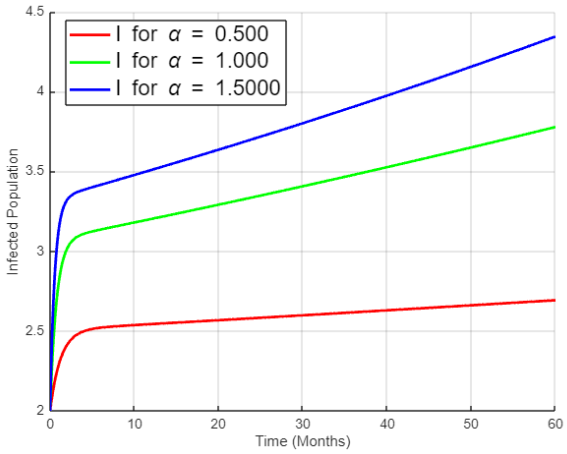

Figure 4 The total number of infected individuals for α = 0.5000, α = 1.0000 and α = 1.5000

4.3 Changes in Recovery Rate (ϒ)

By changing the parameter value of recovery rate, γ, the variation of dynamics can be observed. The simulation results can be compared with varying the parameter values of γ = 0.2857, γ = 0.3929 and γ = 0.5000. The result is shown in Figure 5.

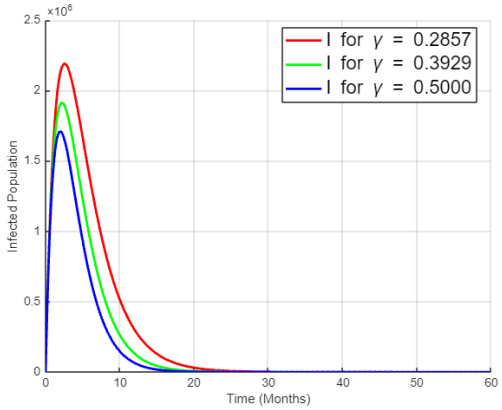

Figure 5 The number of infected individuals for ϒ = 0.2857, ϒ = 0.3929 and ϒ = 0.5000

Figure 5 shows the infected population over time for different values of γ, which represents the recovery rate. The recovery rate is the rate at which infected 47 individuals recover and become susceptible

again. A higher recovery rate (Y) means that individuals are recovering and becoming susceptible more quickly, leading to a decrease in the number of infected individuals. This is reflected in Figure 5, where the blue curve (γ = 0.5000) shows the fastest decline in the infected population, indicating individuals are recovering quickly. The red curve (γ = 0.2857) shows the slowest decline, indicating individuals take longer time to recover. The green curve (γ = 0.3929) falls somewhere in between. The shape of the curves suggests that even with a slower recovery rate (lower γ), the infected population eventually declines.

Conclusion and Recommendations

This study investigates the transmission of influenza A (H1N1) in the Ashanti region of Ghana using the SEIR model, an extension of the SIR model. It includes four classes: susceptible, exposed, infected, and recovered, with parameters for transmission, infection, and recovery rates. The analysis shows that the disease-free equilibrium point (DFEP) is unstable while the endemic equilibrium point (EEP) is stable, depending on the basic reproduction number (R_0). Using the Next-Generation Matrix method and the Routh-Hurwitz Criterion, it concludes that the disease will disappear if R_0 > 1. Numerical simulations with MATLAB's ODE45 highlight the infection rate as critical in disease prevention. The study underscores the importance of epidemiological analysis and mathematical modelling in understanding infectious disease dynamics and developing effective public health strategies.

In the future, refining the SEIR model for H1N1 transmission in the Ashanti region can enhance its accuracy by integrating local infection rates, contact patterns, and recovery rates. Allowing variable transmission (β), latent (α), and recovery (γ) rates will account for behaviour changes and interventions. Adding age-structured compartments and geospatial data will improve predictions. Incorporating adaptive human behaviour, healthcare system constraints, real-time data updates, and scenario analyses will enhance model accuracy and responsiveness. Using historical data and GIS mapping will further refine the model, improving its effectiveness for public health decisions and H1N1 control in the Ashanti region.

Acknowledgement

I'm immensely grateful to God for His blessings, to Dr. Fuaada Mohd Siam for her guidance, and to my family, whose support is invaluable. To my friends, thank you for your encouragement and support.

References

[1] Payne, S. (2017). Chapter 23 - Family Orthomyxoviridae. In S. Payne (Ed.), Viruses (pp. 197–208). Academic Press. https://doi.org/10.1016/B978-0-12-803109-4.00023-4.

[2] Bouvier, N. M., & Palese, P. (2008). The biology of influenza viruses. Vaccine, 26(Suppl 4), D49–D53. https://doi.org/10.1016/j.vaccine.2008.07.039.

[3] Racaniello, V. (2009, April 29). Influenza virus transmission. Virology Blog. https://virology.ws/2009/04/29/influenza-virus-transmission/.

[4] World Health Organization. (2023). Influenza (seasonal). WHO. https://www.who.int/news-room/fact-sheets/detail/influenza-(seasonal)?gclid=CjwKCAiAu9yqBhBmEiwAHTx5pwh2y2Ke3gCKNLeXuVNWV5rkhks23Q30CgHfXfihOK4d5DHjbtBwE

[5] Saunders-Hastings, P. R., & Krewski, D. (2016). Reviewing the history of pandemic influenza: Understanding patterns of emergence and transmission. *Pathogens, 5*(4), 66. https://doi.org/10.3390/pathogens5040066.

[6] Centers for Disease Control and Prevention. (2009). Outbreak of swine-origin influenza A (H1N1) virus infection - Mexico, March-April 2009. *MMWR. Morbidity and Mortality Weekly Report, 58*(17), 467–470.

[7] Center for Disease Control and Prevention. (2009). Update: Novel influenza A (H1N1) virus infection - Mexico, March - May. *Morbidity and Mortality Weekly Report (MMWR), 58*, 585–589.

[8] Cutler, J., Schleihauf, E., Hatchette, T. F., Billard, B., Watson-Creed, G., Davidson, R., Li, Y., Bastien, N., Sarwal, S., & Team, N. S. H. S. I. I. (2009). Investigation of the first cases of human-to-human infection with the new swine-origin influenza A (H1N1) virus in Canada. *Canadian Medical Association Journal, 159*, 159–163. https://doi.org/10.1503/cmaj.090859.

[9] Influenza A (H1N1). (2009). ReliefWeb. https://reliefweb.int/report/austria/influenza-ah1n1-update-81.

[10] Center for Disease Control and Prevention. (2009). Update: Novel influenza A (H1N1) virus infections - Worldwide. *Morbidity and Mortality Weekly Report (MMWR), 58*, 453–458.

[11] Brankston, G., Gitterman, L., Hirji, Z., Lemieux, C., & Gardam, M. (2007). Transmission of influenza A in human beings. *The Lancet Infectious Diseases, 7*(4), 257–265. https://doi.org/10.1016/S1473-3099(07)70029-4.

[12] Coleman, K. K., & Sigler, W. V. (2020). Airborne influenza A virus exposure in an elementary school. *Scientific Reports, 10*(1), 1859. https://doi.org/10.1038/s41598-020-58588-1.

[13] Siston, A. M., Rasmussen, S. A., Honein, M. A., & et al. (2010). Pandemic 2009 influenza A(H1N1) virus illness among pregnant women in the United States. *JAMA, 303*(15), 1517–1525. https://doi.org/10.1001/jama.2010.479.

[14] Okyere, S., Oduro, F., Bonyah, E., & Munkayazi, L. (2013). Epidemiological model of influenza A (H1N1) transmission in Ashanti Region of Ghana, 2012. *Journal of Public Health, 5*, 160–166.